Electronic Supplementary Material (ESI) for Environmental Science: Water Research & Technology.
This journal is © The Royal Society of Chemistry 2020

Electronic Supplementary Information for:

Stable Immobilized Amine Sorbents for Heavy Metal and REE Removal from Industrial Wastewaters

Walter Christopher Wilfong[a,b]*, Brian W. Kail[a,b], Qiuming Wang[a,c], Fan Shi[a,b], Greg Shipley[d], Thomas Tarka[a], and McMahan L. Gray[a]*

[a]National Energy Technology Laboratory, 626 Cochrans Mill Road, P.O. Box 10940, Pittsburgh, PA 15236-09040, USA.

[b]Leidos Research Support Team (LRST), 626 Cochrans Mill Road, P.O. Box 10940, Pittsburgh, PA 15236-09040, USA.

[c]Oak Ridge Institute for Science and Education (ORISE), P.O. Box 117, Oak Ridge, TN 37831, USA.

[d]BioEnergy Development, 4004 Stags Leap Way, Paso Robles, CA 93446

Synthetic and Real Solution Compositions

Table S1: Average metal concentrations of stock solutions for treatment studies determined by a combination of ICP-MS, ICP-OES, and CVAAS (for Hg). Blank fields represent data not reported or analyzed. BDL is below detection limit. * Represent species and concentrations often determined by ICP-OES.

	Metal concentration (ug/L, ppb)							
Metal	**RCRA**	**AMD-PBG**	**FGD**	**Pb-spiked tap**	**AMD-SYN**	**5-REE**	**Detection Limit (ppb)**	**Reporting Limit (ppb)**
B*	811.5	104.36	106092.62	48.53	0	0	11.44	50
Na	60775.04	3103.79	35329.09	37284.58	285289.85	96.22	5.0295	1000
Mg*	BDL	12915.75	511799.6	8020.99	10605.48	BDL	23.80	5000
Al	BDL	6213.2	44.35	20.52	14941.26	27.6	8.2911	1
K	225.15	302.97	8298.77	2013.78	117.43	BDL	52.7573	1000
Ca*	BDL	51918.99	2051000	33703.95	57505.93	BDL	7.84	5000
Sc		1.3	1.22				0.0271	1
Cr	24656.86	1.2	17.09	0.46	5.29	BDL	0.0867	1
Mn	BDL	239.19	1637.19	2.3	52012.06	3.44	0.0443	1
Fe	BDL	71.51	115.96	11.4	273739.76	148.35	3.4323	100
Ni	BDL	56.52	135.92	BDL	BDL	BDL	0.1515	1
Cu	195.81	7.19	4.24	525.82	1.47	1.94	0.0522	0.1
Zn	9.39	79.25	1154.76	162.84	BDL	16.49	0.659	1
As	29282.6	BDL	BDL	BDL			1.1059	1
Se	25230	BDL	178	BDL			1.9448	1
Sr*	BDL	673.91	11540	267.64			0.71	50
Y	BDL	8.36	0.9				0.0012	0.1
Mo	0.25	BDL	12.71	0.87			0.0372	1
Ag	0.28	BDL	0.04	BDL			0.0233	1
Cd	10962.58	0.56	49.39	0.03			0.0738	1

Ba	2.02	2.82	301.29	43.97			0.0842	0.1
La	BDL	5.16	0.23		14.47	46759.82	0.0032	0.01
Ce	BDL	19.81	0.1				0.0024	0.01
Pr	BDL	3	0.02				0.003	0.01
Nd	BDL	14.37	BDL		25	45129.76	0.0722	0.01
Sm	BDL	3.83	0.03				0.0059	0.01
Eu	BDL	0.83	0.08		1.86	53324.16	0.003	0.01
Gd	BDL	3.61	0.03				0.0027	0.01
Tb	BDL	0.41	BDL				0.0035	0.1
Dy	BDL	2.16	0.04		8.77	54457.31	0.0025	0.01
Ho	BDL	0.35	0.01				0.0002	0.01
Er	BDL	0.9	0.03				0.0053	0.01
Tm	BDL	0.09	0.01				0.0004	0.01
Yb	0.02	0.61	0.06		3.75	56667.45	0.0008	0.01
Lu		0.07	0.01				0.002	0.01
Re	0.01	BDL	7.74	BDL			0.0172	1
Pb	35282.37	0.14	0.44	124.61			0.0147	0.1
U	BDL	0.27	32.02	0.03			0.0026	0.1
Hg	33500	0.02	1.74				0.0002	0.00056
pH	*6.2*	*3.6*	*6.7*	*5.7*	*2.6*	*5.3*		

Table S2: Anion concentrations for FGD and AMD-PBG wastewaters, excluding the potential oxyanionic forms of other metals present. *Four solutions were used: Each of 5.0 mM Eu and Cd mixed with either 5 mM NO_3^- or SO_4^{2-}. SO_4^{2-} and NO_3^- concentrations correspond to those within the Eu and Cd solutions that contain only that specific anion.

	Metal Concentration (mg/L)			
Anion	**FGD**	**AMD-PBG**	**For Relative Max Uptake***	**Detection Limit**
PO_4^{3-}	BDL	not tested		0.5-1.0
NO_3^-	104.59	BDL	465	0.5-1.0
Br^-	10.75	not tested		0.5-1.0
SO_4^{2-}	1356	202.1	345	0.5-1.0
NO_2^-	BDL	BDL		0.5-1.0
Cl^-	7297	2.3	350-550	0.5-1.0
F^-	0.77	BDL		0.5-1.0

Analytical Procedures

Metal concentrations for all samples were analyzed using a Perkin Elmer Nexion 300D Inductively Coupled Plasma Mass Spectrometer (ICP-MS) operated in kinetic energy discrimination (KED) mode using He as the collision gas. Samples were analyzed according to EPA method 6020. Aqueous samples of treated and stock solutions were diluted 100-fold for major element concentrations (Mg, Ca, Na, etc.) and 10,000-fold for minor rare earth (La through Yb) and some heavy element concentrations in 2% HNO_3 prior to analysis, which stabilizes the solution and dissolves any precipitates. For general validation of ICP-MS sample analysis repeatability, standard reference materials (SRM) were analyzed in parallel with each batch of the study samples and included trace metals in both drinking water (High Purity Standards) and preserved natural waters T221 and T223 (United States Geological Survey). Data accuracy was determined and ensured using recovery of SRM and spiked sample recovery while precision was calculated based on duplicate measurements of samples.

Solution analysis by Inductively Coupled Plasma Optical Emission Spectroscopy (ICP-OES) was performed according to EPA Method 6010D, using an Optima 7300 DV (Perkin Elmer, Waltham, MA) dual-view spectrometer equipped with solid state SCD detectors. Sample solutions were nebulized using a glass Seaspray concentric nebulizer and a glass Baffled Cyclonic spray chamber (Glass Expansion – Pocasset, MA) using 5 ppm yttrium as an online internal standard. Calibration standards were purchased from Inorganic Ventures (Christiansburg, VA) and are traceable to NIST standard reference materials.

Analysis of Hg by Cold Vapor Atomic Absorption Spectroscopy (CVAAS) was performed according to EPA method 245.7, using a Cetac M-8000 Quick Trace Cold Vapor Atomic Fluorescence Mercury Analyzer. Generally, samples are oxidized with potassium bromate/potassium bromide; pre-reduced with NH_2OH-HCl then reduced with $SnCl_2$ to convert Hg(II) to volatile Hg(0); separation of Hg(0) by passing the sample through a liquid-gas separator under high purity Ar; analysis by atomic fluorescence spectrometry at 253.7 nm. Samples were diluted prior to analysis, when necessary, using 1% HCl.

DRIFTS Analysis of PES-X-100 Sorbents

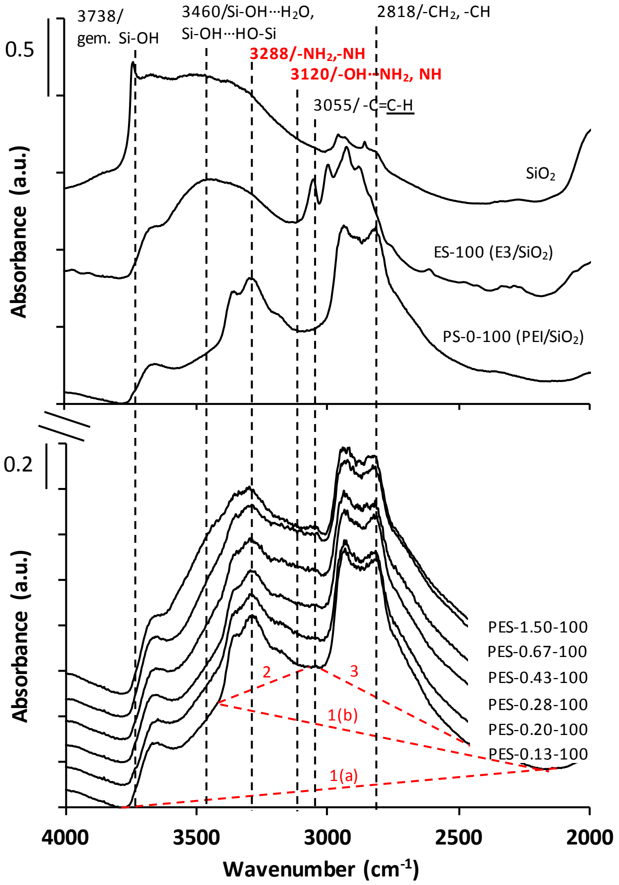

Fig. S1: IR absorbance spectra of pretreated (120 °C, N_2, 30 min) fresh PES-X-100 immobilized amine sorbents collected at 50 °C, including pure SiO_2, E3/SiO_2, and PEI/SiO_2 as references. Note, PS-0-100 contains no E3 crosslinker. Absorbance=log(1/I), where I is the single beam spectrum of interest. The red dashed lines highlight spectral baselines from which IR absorbance ratios were calculated.

Fig. S1 shows the IR absorbance spectra [Abs.=log(1/I)] of pretreated fresh PES-X-100 sorbents. Characteristic features of impregnated PEI are evident by N-H stretching bands of amines at 3355 and 3288 cm^{-1} and C-H stretching bands of alkyls at 2932 and 2818 cm^{-1}. E3 produced the familiar aromatic C-H stretch at 3054 cm^{-1}, whose weak intensity strengthens with increasing E3/PEI ratio. Reduced 3738 cm^{-1} intensity for all sorbents relative to that of pure SiO_2 confirms the anchoring of surface-bound organics onto silica's unbound geminal Si-OH groups. Reduction in the broad band between 3600 and 3200 cm^{-1}, centered around 3460 cm^{-1}, from PES-0.13-100 to PES-0.43-100 shows interaction of silica's hydrogen-bonded Si-OH species with predominantly impregnated PEI rather than E3. Comparing the spectra of PS-0-100 (no E3) and ES-100 (no PEI) confirms this behavior. Further increasing the E3/PEI ratio for PES-0.67-100 and PES-1.5-100 reduced the amount of PEI attached to hydrogen-bonded Si-OH. This is evidenced by the strengthened and broadened 3600-3400 cm^{-1} IR features. IR intensity generated between 3200 and 3000 cm^{-1} displays features similar to those we previously observed for pure tetraethylenepentamine (TEPA)-E3 polymer particles,[1] and is attributed to the formation of hydrogen-bonded -OH···amine species. Crosslinking of PEI with E3 generated C-N (E3-PEI) linkages with pendant -OH groups that interacted with neighboring $-NH_2$ and -NH groups. These interactions provided the sorbents with added amine leach resistance and will likely serve as unique binding sites during metal uptake tests. Note, because of the relatively weak intensities of C-N stretching bands compared to those of overlapping C-O-C (E3) and Si-O-Si vibrations (SiO_2), crosslinked PEI-E3-PEI species could not be directly observed in the IR spectra.

Fig. S2 plots key IR absorbance intensity ratios derived from the spectra in Fig. S1 and amine efficiencies [mol CO_2/mol N (PEI, $-NH_2$ and -NH)] calculated from CO_2 capture measurements to further clarify structure-performance relationships. Because the amount of PEI varies, IR ratios were calculated from the 2818 C-H band that is primarily associated with PEI. Expectedly, the drop in the 3288 cm^{-1} amine/2818 cm^{-1} alkyl (PEI) ratio was inversely related to the growth in the 3120/2818 band as PEI $-NH_2$ and -NH groups reacted to form *E3*-CH_2-CH**(-OH)-**CH_2-NH-*PEI* or *E3*-CH_2-CH**(-OH)-**CH_2-N-*PEI* species, respectively. Whereas most changes in the IR ratios were observed up to X=0.43, only a 32.5% loss of the initial amine efficiency was displayed.

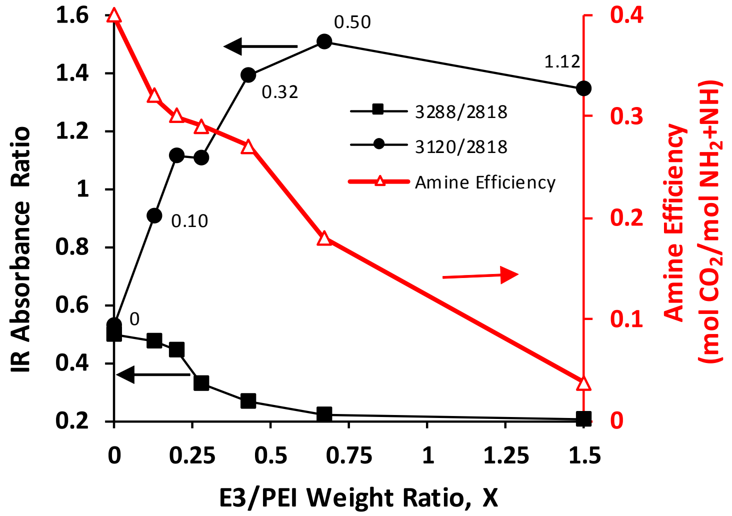

Fig. S2: IR absorbance ratios for the spectra in Fig. 2 and amine efficiencies of PES-X-100 sorbents. Baseline assignment for determining IR band height and ratios, according to Fig. 2 are as follows: 3120 – 1(a), 3288 – 2, 2818 – 3. Interpretation of the results involving the 3120/2818 ratio measured from baseline 1(b) do not significantly vary from those involving 1(a).

This was followed by an additional 58.5% decline up to X=1.5. Amine efficiency here directly measured the effective utilization of PEI's -NH_2 and -NH groups to adsorb CO_2. Greater reduction in the amine efficiency relative to the change in E3/PEI ratio, meaning Δamine effic./ΔX, from X=0 to 0.43 (-0.30) compared to from X=0.43 to 1.5 (-0.22) was apparent. We postulate this is owed to simultaneous loss of amine sites as the PEI-E3-PEI network is formed and a combination of the following effects: (i) blockage of CO_2 to amine sites contained within the new network and (ii) conversion of more basic, unreacted -NH_2 and -NH into less basic and likely hindered, crosslinked -NH and -N, respectively.

Adsorption of Species from Single-Element RCRA and AMD-SYN Solutions

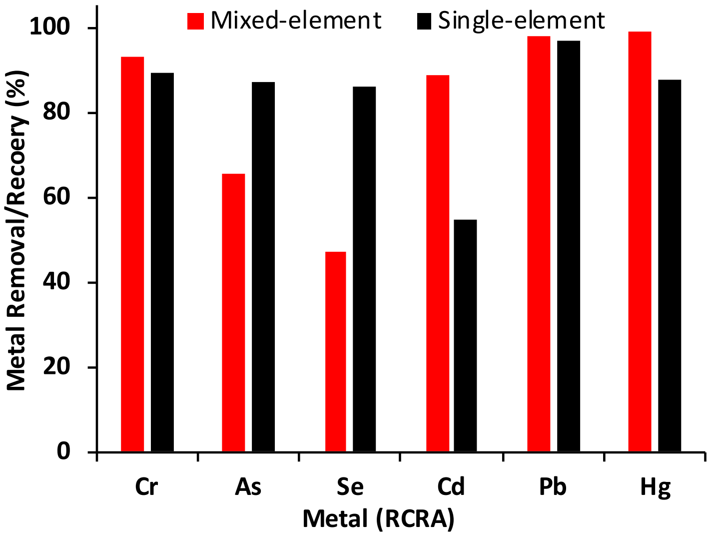

Fig. S3: Metal adsorption of the six RCRA metals by PES-0.43-500 from ~25 ppm mixed- and single-element solutions. Note, the concentration of Pb was about 96 ppm for the single-element test.

Mixtures of Cr, As, Se, Cd, and Hg did not generate precipitates after aging. This contrasts precipitation observed for the 6-element solution with Pb. Therefore, we expect highly efficient Pb removal plus that of the other metals by PES-0.43-500 generally precludes physical filtration as a mechanism of metal capture from the 6-element mixture by all sorbents.

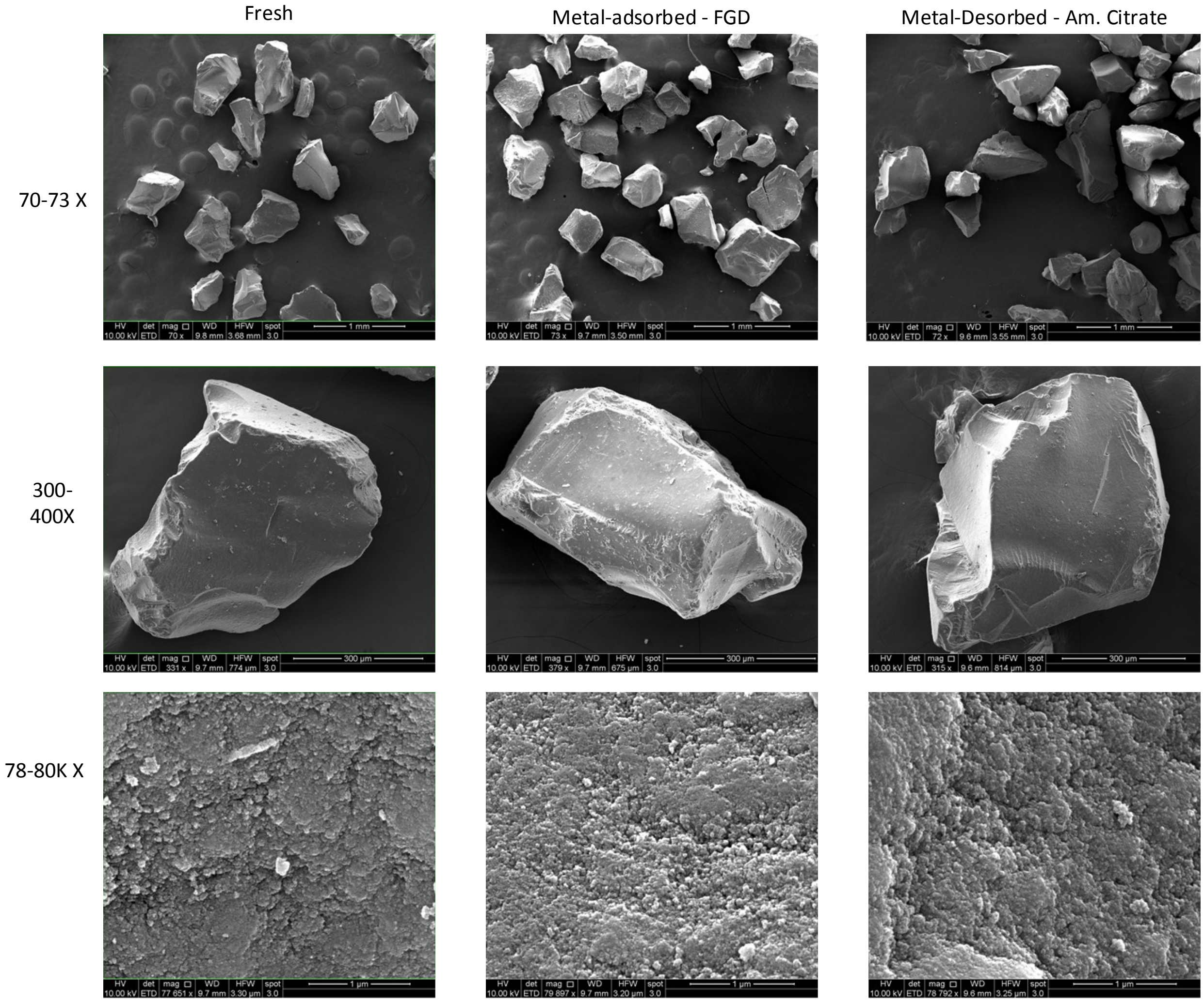

Figure S4: SEM images of PES-0.43-500 before and after metal adsorption from FGD, plus after metal desorption with ammonium citrate-based buffer.

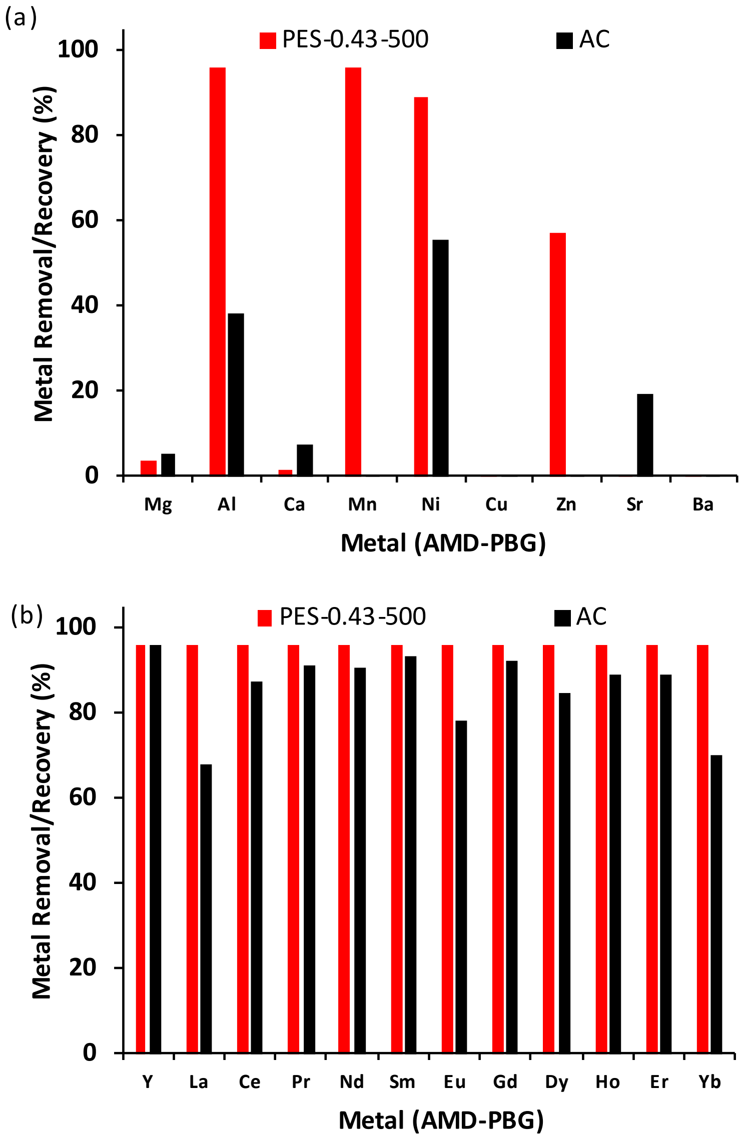

Fig. S5: Treatment of AMD-PBG with PES-0.43-500 and Calgon activated carbon (AC), type BG HHM sieved to between 425 and 600 µm.

DRIFTS Spectra of PES-0.43-500 with Adsorbed Metals

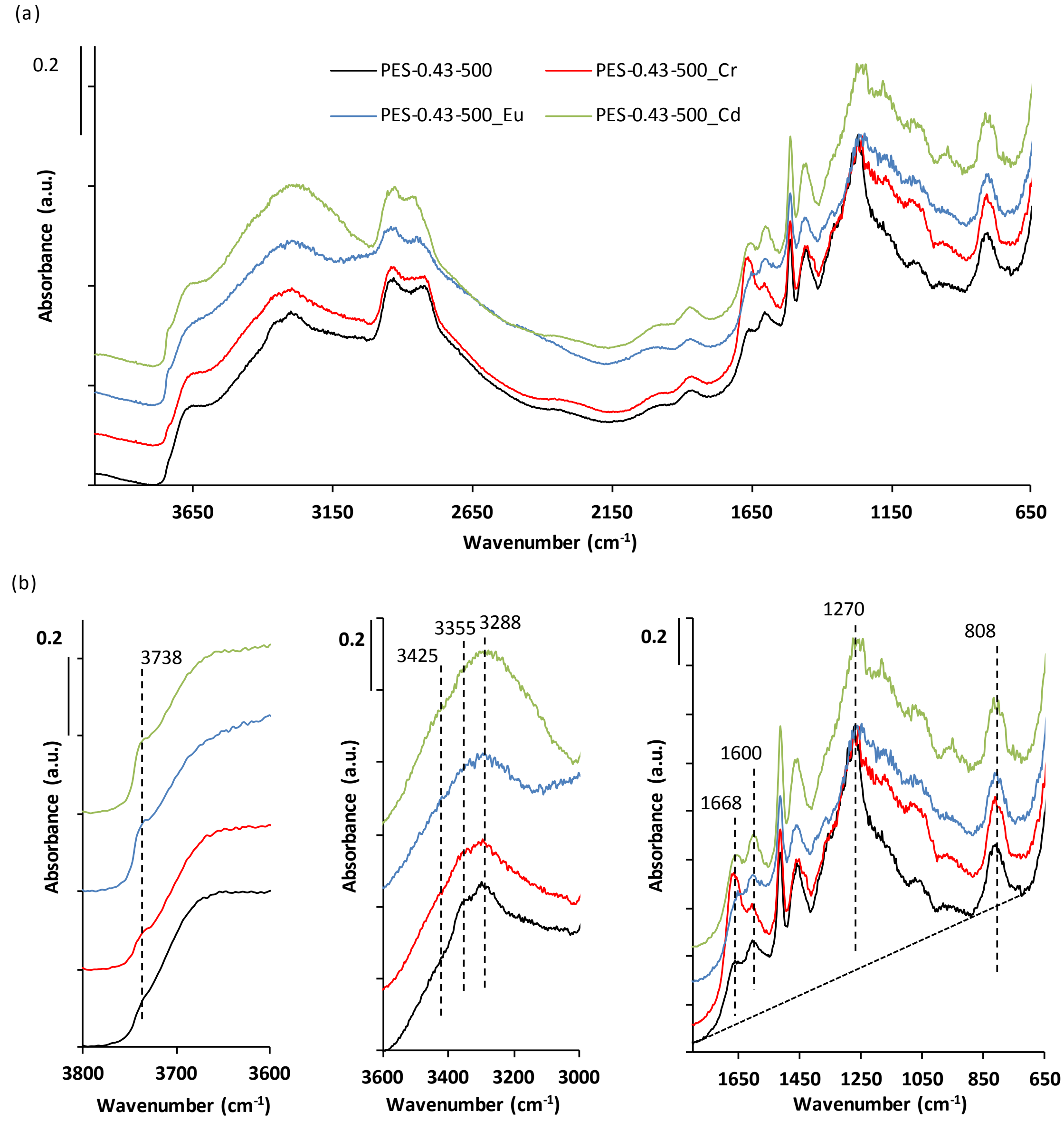

Fig. S6: DRIFTS absorbance spectra of fresh and metal-adsorbed PES-0.43-500 sorbents taken at 50 °C. Absorbance=log(1/I), where I is the single beam spectrum of each sample pretreated at 120 °C in N_2 for 30 min then cooled down.

Oxidation of amines to amides/imides by chromate in the PES-0.43-500_Cr spectrum is evidenced by generation of the prominent 1668 C=O band paralleled with slight attenuation of the low-frequency C-H stretching vibration.[2] Chelation of Cd^{2+} and Eu^{3+} by the $-NH_2$ and -NH groups of PEI in the bulk network is manifested in the broadened amine stretching features and suppression of the 3355 cm^{-1} N-H and C-H stretching band intensities. We ascribe the slight emergence of geminal Si-OH (3738 cm^{-1}) and H-bonded Si-OH···OH-Si (3425 cm^{-1}) groups along with weakened Si-O-Si band (1270 cm^{-1}) to the detachment of PEI from the Si-OH surface. Note that the 3425 cm^{-1} band could result from H_2O coordinated to the amine-metal complexes.[3] We postulate that these detached amine groups at the E3-PEI/SiO_2 surface layer partially contributed to metal adsorption. We expect reattachment of detached PEI to silica upon release of the adsorbed metals with a buffer solution. Overall greater changes in the IR features of PES-0.43-500_Eu (5.89 wt% Eu) than of PES-0.43-500_Cd (8.07 wt% Cd) relative to PES-0.43-500 correspond to presumably stronger Eu^{3+}···amine acid-base interactions; Eu pKa value 3-4, Cd pKa value 9.4. [4, 5]

Kinetic Uptake Test

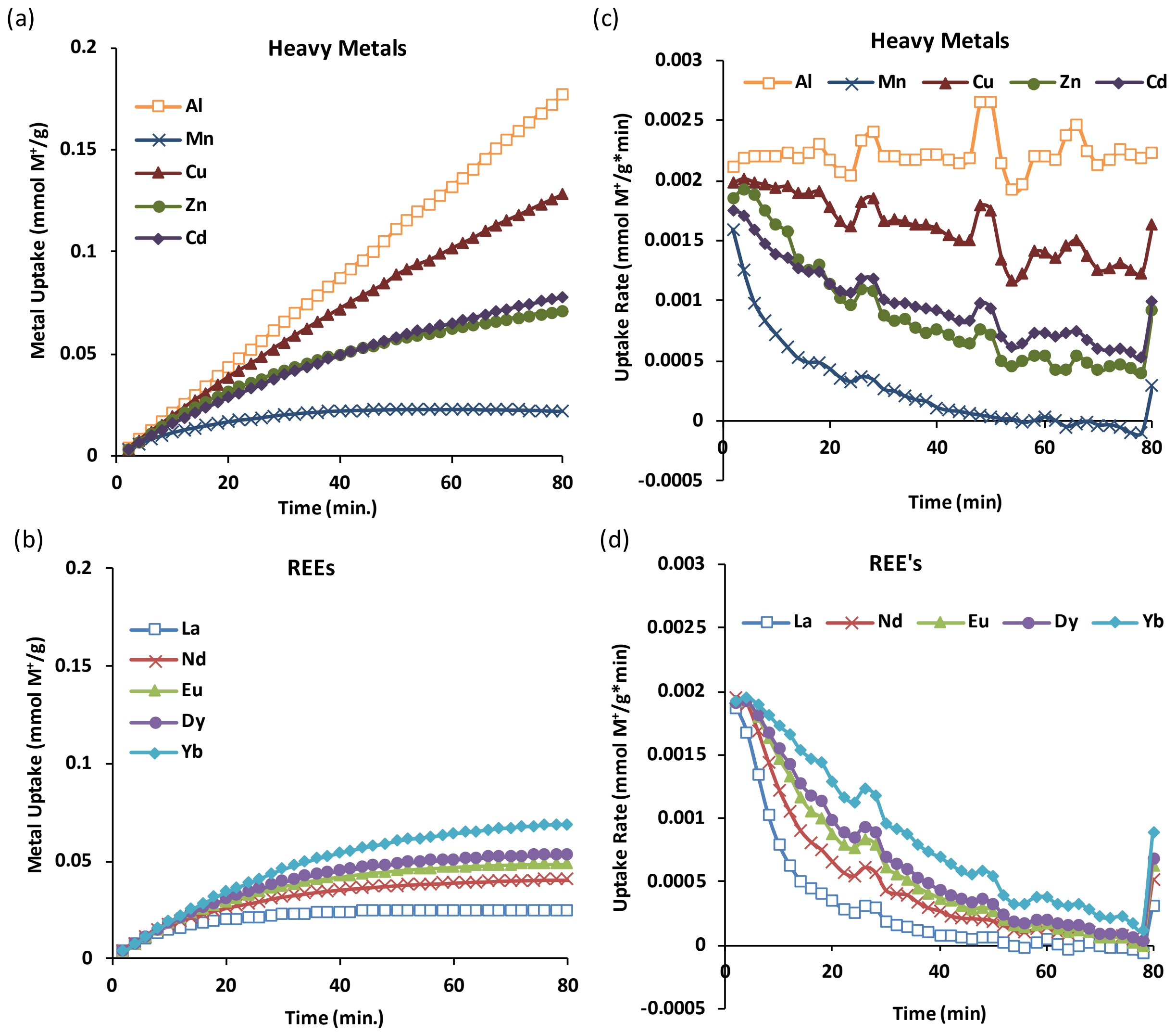

Figure S7: Transient profiles, showing uptake capacity (a) and (b) and uptake rate (c) and (d) of heavy metals and REEs as functions of time. The test was performed by flowing 40 mL of a 10.0 mM equimolar metal solution (natural pH 3.9) over 0.5 g of PES-0.43-500 at 0.5 mL/min and sampling every 1 mL (2 min).

Table S3: Uptake capacity of PES-0.43-500 (0.5 g) for cation metal removal from 40 mL of a 10.0 mM, equimolar solution.

	Aqueous Ionic Radii	*pKa*	Uptake Capacity	
Metal	(pm)[6;7]	(M^+-OH···***H***)[4]	(mg/g)	(mmol M^+/g)
Al^{3+}	NA; 50	4.6	4.8	0.177
Cu^{2+}	NA; 72	7.7	8.2	0.129
Zn^{2+}	NA; 70	5.5	4.7	0.071
Mn^{2+}	NA; 80	8.6	1.2	0.022
Cd^{2+}	NA; 91	9.4	8.8	0.078
Total			27.6	0.478
Yb^{3+}	101.0; NA	3.53	11.9	0.069
Dy^{3+}	107.5; 98	3.65	8.7	0.053
Eu^{3+}	112.0; 106	3.98	7.4	0.049
Nd^{3+}	117.5; 108	4.64	5.8	0.040
La^{3+}	125.0; 114	5.88	3.4	0.024
Total			37.2	0.235

References

1. Wilfong, W. C.; Kail, B. W.; Bank, T. L.; Howard, B. H.; Gray, M. L., Recovering Rare Earth Elements from Aqueous Solution with Porous Amine-Epoxy Networks. *ACS Appl. Mater. Interfaces* **2017,** *9*, (21), 18283-18294.
2. Srikanth, C. S.; Chuang, S. S. C., Spectroscopic Investigation into Oxidative Degradation of Silica-Supported Amine Sorbents for CO2 Capture. *ChemSusChem* **2012,** *5*, (8), 1435-1442.
3. Buckingham, D. A.; Jones, D., Infrared Spectra of Cobalt(III) Triethylenetetramine Complexes. *Inorg. Chem.* **1965,** *4*, (10), 1387-1392.
4. Yu, D.; Du, R.; Xiao, J.-C.; Xu, S.; Rong, C.; Liu, S., Theoretical Study of pKa Values for Trivalent Rare-Earth Metal Cations in Aqueous Solution. *The Journal of Physical Chemistry A* **2018,** *122*, (2), 700-707.
5. Jackson, V. E.; Felmy, A. R.; Dixon, D. A., Prediction of the pKa's of Aqueous Metal Ion +2 Complexes. *The Journal of Physical Chemistry A* **2015,** *119*, (12), 2926-2939.
6. D'Angelo, P.; Zitolo, A.; Migliorati, V.; Chillemi, G.; Duvail, M.; Vitorge, P.; Abadie, S.; Spezia, R., Revised Ionic Radii of Lanthanoid(III) Ions in Aqueous Solution. *Inorg. Chem.* **2011,** *50*, (10), 4572-4579.
7. Marcus, Y., Ionic radii in aqueous solutions. *Chem. Rev.* **1988,** *88*, (8), 1475-1498.